Composites Science and Technology, Vol. 64, no. 7-8, pp. 1011-1020 (2004)

Comparison of Two Models of SWCN Polymer Composites

G.M. Odegard[a] , R.B. Pipes[b], P. Hubert[c]

[a]*National Institute of Aerospace, 144 Research Drive, Hampton, VA 23681*
[b]*University of Akron, Akron, Ohio*
[c]*McGill University, Montreal, Canada*

Abstract

Two approaches for predicting elastic properties of SWCN/polymer composites, equivalent-continuum modeling and the self-similar approach, are presented and compared in terms of assumptions and ranges of validity. Both models incorporate information about molecular interactions at the nanometer length scale into a continuum-mechanics based model. It is shown that the two approaches can predict elastic properties of SWCN/polymer composites in a combined range spanning dilute to hyper-concentrated SWCN volume fractions. In addition, the predicted Young's moduli for a SWCN/polymer composite determined using both approaches are shown to be consistent.

Keywords: Carbon nanotubes, volume fraction, representative volume element, helical array, lattice dynamics, molecular mechanics, elastic properties.

1. Introduction

The incorporation of single-walled carbon nanotubes (SWCN) in a polymeric matrix to develop the next generation of high performance composite materials has attracted significant attention since their discovery more than a decade ago [1, 2]. Many studies have been performed that address the direct incorporation of individual SWCN into a polymer matrix [3-13]. Other studies focus on the development of micro-fibers, which are assembled from arrays of aligned SWCNs [14-18]. In order to facilitate the development of SWCN-reinforced polymer composites, models must be developed to predict the bulk mechanical properties of the composite as a function of atomic structure and interaction. Fig. 1 clearly illustrates the challenge of geometric scale in linking the nanoscale to the macroscale - 12 orders of magnitude.

Even though numerous micromechanical models have been developed to predict the macroscopic behavior of composite materials reinforced with typical carbon fibers and fiber structures [19, 20], the direct use of these methods for nanotube composites is complicated by the significant scale difference of the SWCN as compared to the typical carbon fiber. While individual atomic interactions at the polymer-reinforcement interface in traditional composites constitute a small fraction of the overall periodic structure, the atoms in a periodic structure of a SWNT composite are significant in both volume and contribution to overall mechanical properties [21]. Therefore, a new generation of reliable modeling strategies are required to

predict overall mechanical properties of SWCN composites that incorporate chemistry-based or physics-based modeling tools.

Recently, two methods have been proposed for modeling the mechanical behavior of SWCN composites. Odegard *et al*. [21] utilized molecular mechanics [22] to model a specific polymer-nanotube interaction and to construct a homogeneous, equivalent-continuum reinforcing element consisting of a SWCN surrounded by a cylindrical volume of polymer. Classical micromechanics analyses were carried out to determine effective bulk properties of the equivalent-continuum reinforcing element embedded in a continuous polymer. This process accomplished the desired objective of representing the nano-scale interactions between polymer and SWCN, while at the same time providing a consistent and rigorous methodology for determining continuum properties for the composite. In the second approach, Pipes and Hubert [23, 24] used lattice dynamics to model an array of SWCNs. A model of a composite was constructed in which the SWCN arrays were embedded into a polymer matrix. This composite was subsequently used in a series of self-similar concentric-cylinder models to build an overall model of a micro-fiber. The importance of this approach is the potential to model a SWCN/polymer composite in which the SWCN orientation and atomic interactions between adjacent SWCNs and are taken into consideration for relatively high SWCN volume fractions.

Since the two modeling strategies accomplish the same goal, that is, prediction of mechanical properties of nanotube composites, using two vastly different approaches, direct comparison for an individual material offers an opportunity for model validation and a clear picture of the expected mechanical behavior for a wide range of length scales and SWCN volume fractions. In this paper, the two models are directly compared in terms of their assumptions, ranges of applicability, and predicted Young's modulus for a SWCN/polymer composite.

2. Modeling approaches

In this section the two modeling approaches are briefly described. The procedure for predicting the longitudinal Young's modulus of a SWCN/polymer composite is presented for both methods.

2.1. Equivalent-continuum modeling

The constitutive properties of the nanotube/polymer composite material were predicted based on the method developed by Odegard *et al*. [21, 25]. This method relies on an equivalent-continuum modeling technique [26] that is used to predict the bulk mechanical behavior of nano-structured materials. In summary, the method consists of four major steps: establishing representative volume elements (RVEs) for the molecular and equivalent-continuum models, deriving and equating potential energies of deformation for both models subjected to identical boundary conditions, establishing a constitutive relationship for the equivalent-continuum model, and using traditional micromechanics techniques to determine larger-scale properties of the composite. Each step of the modeling is described below. Further details of the modeling may be found elsewhere [21].

In order to establish the RVE of the molecular model, and thus the equivalent-continuum model, the molecular structure was determined. A Molecular Dynamics (MD) simulation [21] was used

to generate the equilibrium structure of a nanotube/polymer composite, which consisted of a (6,6) single-walled nanotube and five PmPV [poly(m-phenylenevinylene) substituted with octyloxy chains] oligimers, each ten repeating units in length. The initial structure was constructed by placing the nanotube at the center of the MD cell, and by inserting the PmPV molecules at random, non-overlapping positions within the MD cell. The molecular structure for a single time increment for an equilibrated system was used as the RVE of the molecular model (Fig. 2). The RVE of the equivalent-continuum model was chosen to be a solid cylinder of the same dimensions as the molecular model RVE. The equivalent-continuum model will be referred as the effective fiber for the remainder of this paper.

For the second step, the potential energies of deformation for the molecular model and effective fiber were derived and equated for identical loading conditions. The bonded and non-bonded interactions of the atoms in a polymeric molecular structure can be quantitatively described by using molecular mechanics [22]. The forces that exist for each atomic interaction, as a result of the relative atomic positions, are described by a force field. These forces contribute to the total potential energy of the molecular system. The potential energy for a molecular system is described by the sum of the individual energy contributions of each type of atomic interaction. For the SWCN/polymer system considered in this study, the total potential energy of the molecular model is

$$U^m = \sum U^r\left(k_r\right) + \sum U^\theta\left(k_\theta\right) + \sum U^{vdW}\left(k_{vdW}\right) \tag{1}$$

where U^r, U^θ, and U^{vdw} are the energies associated with covalent bond stretching, bond-angle bending, and van der Waals interactions, respectively (see Fig. 3), and the summations are for all of the corresponding interactions in the molecular model. The energy terms in Eq. (1) are a function of the force constants (k_r, k_θ, and k_{vdw}) that were chosen for this particular molecular system [21].

An equivalent-truss model of the RVE was used as an intermediate step to link the molecular and equivalent-continuum models. Each atom in the molecular model was represented by a pin-joint, and each truss element represented an atomic bonded or non-bonded interaction. The potential energy of the truss model is

$$U^t = \sum U^a\left(E^a\right) + \sum U^b\left(E^b\right) + \sum U^c\left(E^c\right) \tag{2}$$

where U^a, U^b, and U^c are the energies associated with truss elements that represent covalent bond stretching, bond-angle bending, and van der Waals interactions, respectively, and the summations are for all of the corresponding interactions in the equivalent-truss model. The energies of each truss element are a function their Young's modulus, E. Because of the mathematical similarity of Eqs. (1) and (2), the moduli of the truss elements were determined from the molecular mechanics force constants. Therefore, the total potential energies of the molecular model and the equivalent-truss model are equal for identical loading conditions. For the nanotube/polymer composite, the equivalent-truss model is shown in Fig. 2.

The potential energy (or strain energy) of the homogeneous, linear-elastic, effective fiber is

$$U^f = U^f\left(\mathbf{C}^f\right) \tag{3}$$

where $\mathbf{C}^f$ is the elastic stiffness tensor of the effective fiber. Equating Eqs. (1) - (3) yields

$$U^f = U^t = U^m \tag{4}$$

Eq. (4) relates the elastic stiffness tensor of the effective fiber to the force constants of the molecular model.

The third step in the modeling technique involved establishing a constitutive equation for the effective fiber. Since the values of the elastic stiffness tensor components were not known *a priori*, a set of loading conditions were chosen such that each component was uniquely determined from Eq. (4). Examination of the molecular model (Fig. 2) revealed that it was accurately described as having transversely isotropic symmetry, with the plane of isotropy perpendicular to the long axis of the nanotube.

There are five independent elastic constants required to determine the entire set of elastic constants for a transversely isotropic material. In this study, five independent elastic constants were determined by employing a technique adapted from the approach of Hashin and Rosen [27]. These elastic constants are: the transverse shear modulus, G_T^f, transverse bulk modulus, K_T^f, longitudinal shear modulus, G_L^f, longitudinal Young's modulus, E_L^f, and the longitudinal elastic stiffness component, C_L^f, where the superscript *f* denotes effective fiber. The longitudinal properties are associated with the direction parallel to the longitudinal axis of the nanotube, and the transverse properties are associated with the transverse plane of isotropy (see Fig. 2).

Each of the five elastic constants of the effective fiber were determined from a single boundary condition applied to both equivalent-truss and effective-fiber models (using Eq. (4)). Therefore, for each applied boundary condition, one elastic constant of the effective fiber was uniquely determined. The calculated values of the five independent parameters for the effective fiber are listed in Table 1.

Overall constitutive properties of the dilute and unidirectional SWCN/polymer composite were determined with the micromechanical-based Mori-Tanaka method [28, 29] by using the mechanical properties of the effective fiber and the bulk polymer matrix material (Fig. 4). The layer of polymer molecules that are near the polymer/nanotube interface were included in the effective fiber, and it was assumed that the matrix polymer surrounding the effective fiber had mechanical properties equal to those of the bulk polymer. Because the bulk polymer molecules and the polymer molecules included in the effective fiber are physically entangled, perfect bonding between the effective fiber and the surrounding polymer matrix was assumed. The bulk polymer matrix material had a Young's modulus and Poisson's ratio of 7.2 GPa and 0.3, respectively. The properties of the composite with aligned nanotubes were calculated for nanotube lengths of 500 nm.

The maximum nanotube volume fraction that can be obtained with this approach is limited by the maximum effective-fiber volume fraction that can be used in the micromechanics analysis. For a hexagonal packing arrangement, the maximum effective-fiber volume fraction is 90.7%. While the nanotube and effective fiber lengths are equal, the nanotube volume fraction is 58.8% of the effective-fiber volume fraction if it is assumed that the nanotube volume is a solid cylinder with a diameter of 1.38 nm, which is just large enough to completely fill in the volume not occupied by polymer molecules (Fig. 2) in the effective fiber. Therefore, the maximum nanotube volume fraction that can be obtained by this modeling approach is 53.3%.

A restriction of the model is that the maximum packing fraction of the SWCN is restricted by the diameter of the RVE due to the cylindrical volume of polymer surrounding the SWCN within the heterogeneous truss model. The range in validity of the model can, however, span a significant range in SWCN volume fraction when the orientation state corresponds to collimation.

2.2. Self-similar approach

The constitutive properties of the nanotube/polymer composite material were also predicted using the self-similar method developed by Pipes and Hubert [23, 24], which is illustrated in Fig. 5 and summarized in Table 2. The self-similar analysis consists of three major steps. In the first step, a helical array of SWCNs is assembled. The geometric properties of the SWCNs are listed in Table 3, which was determined from the SWCN array and representative hexagonal image as illustrated in Fig. 6. This array is termed the SWCN nano-array where ninety-one SWCNs make up the cross-section of the helical nano-array. Given that the SWCN is a discontinuous reinforcement, twisting the nano array provides a second mechanism of load transfer, typical of a staple textile yarn. However, the angle of twist has been shown to have a significant effect upon the axial stiffness of the array [5]. Therefore, the helical angle (α) of the SWCN nano-array was chosen as 10^{o}.

The SWCN nano-arrays is surrounded by a polymeric matrix and assembled into a second twisted array, termed the SWCN nano-wire, with a resulting diameter and nanotube volume fraction of 1.69×10^{-7} m and 54.6%, respectively. SWCN nano-wires are then impregnated with a polymer matrix and assembled into the final helical array – the SWCN micro-fiber with a diameter and nanotube volume fraction of 1.93×10^{-6} m and 33.2%, respectively. Fig. 5 illustrates the assembly of the three arrays into the micro-fiber. The tangent of the helical angle for the SWCN nano-arrays and nano-wires were also 10^{o}. The self-similar geometries described in the nano-array, nano-wire, and micro-fiber allow the use of the same mathematical and geometric model for all three geometries [23]. It is assumed that the nano-array is perfectly bonded to the impregnating polymer.

The layered cylinder analysis replaces each of the three arrays with a layered cylinder with effective layer properties and with the tangent of the helical angle varying linearly with radial position in order to represent a twist in the array (Fig. 7). The helical angle of each layer is distinct and is determined by its radial position from the cylinder axis. For the nano-array, it is assumed that the discontinuous nanotubes are collimated and lay within the cylindrical layer surface. The volume fraction of carbon nanotube is taken as 79%.

The layer properties of the nano-array crystal (Table 4) were obtained from the work of Popov *et al*. [30] and from estimates by the authors. The longitudinal Young's modulus, E_{L}^{s}, transverse Young's modulus, E_{T}^{s}, and the Poisson's ratio, ν_{LT}^{s}, were obtained for a crystal composed of SWCN with a diameter of 1 nm. Values for the longitudinal shear modulus, G_{LT}^{s}, transverse shear modulus, G_{NT}^{s}, and Poisson's ratio, ν_{NT}^{s}, were assumed by the authors. The superscript *s* denotes the self-similar approach. A value of 894 GPa was taken as the Young's modulus of SWCN [23].

The concentric layers were assumed to be perfectly bonded together. Continuity of radial stress and radial displacement at the layer interfaces is assured. Finally, the cylinder was subjected to combination of uniform extensional strain, w_0 (m/m), torsional shearing strain/radius, v_0 (rad./m), torque, T (N-m), and axial force, F (N). For the nano-wire and micro-fiber, the elastic properties of each layer of the multi-layered cylinder were determined by using micromechanics relations from Bogetti and Gillespie [31].

Perhaps the most interesting aspect of this approach is that it provides a methodology to begin at maximum SWCN volume fraction and move to lower volume fractions in a systematic way. It further treats the SWCN interaction in the absence of a polymer phase in the nano-array and the element of twist is introduced in anticipation of the need for enhanced load transfer to achieve nano-array strengths representative of the SWCN.

3. Model comparison

Consider the two approaches and their unique starting points in the length-scale space as shown in Fig. 8. Here the two approaches are clearly compared over the length-scale range of $1.8\text{x}10^{-9}$ m to $2.2\ \text{x}10^{-5}$ m. In Fig. 9, the relationship between length-scale and volume fraction is illustrated. The range of the equivalent-continuum model nanocomposite begins at a nanotube volume fraction of 58% and a length scale of $1.8\text{x}10^{-9}$ m. Even though the effective fiber is a nanoscale element, micromechanics is used to predict the properties of the SWCN/polymer composite over the range of dilute to hyper-concentrated volume fractions less than or equal to 53.3% (Table 5). Note that this model is bounded in scale by $1.8\text{x}10^{-9}$ m and nanotube volume fractions less than 53.3% (shaded area in Fig. 9).

Next we consider the self-similar approach and the four distinct geometric forms can be seen in Fig. 8. The nano-array, nano-wire, microfiber and lamina are clearly shown to span the volume fraction range from 78% to 32% and length scale from $1.8\text{x}10^{-8}$ to $2.0\text{x}10^{-5}$ m. Unlike the equivalent-continuum modeling approach, the self-similar approach utilizes specific geometries that are self-similar. In the initial state, the nano-array is at a volume fraction of 78% and scale of $1.8\text{x}10^{-8}$ m. The self-similar approach is confined to the hyper-concentrated regime, and it is interesting to note that the nanotube volume faction is systematically reduced from 78% to 32% as the length scale is increased from $1.8\text{x}10^{-8}$ to $2.0\text{x}10^{-5}$ m.

Fig. 10 shows the normalized Young's modulus of the composite as predicted by the two approaches. The normalization factor, E_{nanotube}, has a value of 894 GPa, as described in the previous section. Clearly the two analyses are consistent and there is a region of overlap in volume fractions of 25-53.3%. This is true in spite of the fact that the micro-fiber contains elements each of which posses an angle of twist of 10º while the equivalent-continuum model results are for 0º fiber orientation. In addition, it is clear from Fig. 10 that the predicted Young's modulus of the nanostructured composite follows a linear trend with respect to the SWCN volume fraction. This is the same trend seen in rule-of-mixtures predictions for graphite and glass-reinforced polymer composites.

For both approaches, there is a reduction in normalized Young's modulus as compared to the classical rule-of-mixtures. This can be shown using the well-known Voigt model [32] assuming the moduli of the nanotube and the matrix as 894 GPa and 7.2 GPa, respectively. For both approaches, the reduction is about 15% over the entire range of volume fractions.

3. Conclusions

Two approaches for predicting elastic properties of SWCN/polymer composites, equivalent-continuum modeling and the self-similar approach, have been presented. In both cases, the model incorporates information about molecular interactions at the nanometer length scale into a continuum-mechanics based model. The two methods have been compared in terms of assumptions and ranges of validity. It has been shown that the two approaches can predict elastic properties of SWCN/polymer composites in a combined range spanning dilute to hyper-concentrated SWCN volume fractions. The predicted Young's moduli for a SWCN/polymer composite determined using both approaches were shown to be consistent. In addition, for both approaches, there is a reduction in predicted Young's modulus compared to the classical rule-of-mixtures of about 15%.

References

1. Iijima S. Helical Microtubules of Graphitic Carbon. Nature, 1991; 354: 56-58.
2. Thess A, Lee R, Nikolaev P, Dai H, Petit P, Robert J, Xu C, Lee Y H, Kim S G, Rinzler A G, Colbert D T, Scuseria G, Tomanek D, Fischer J E, Smalley R E. Crystalline Ropes of Metallic Carbon Nanotubes. Science, 1996; 273: 483-487.
3. Ajayan P M, Schadler L S, Giannaris S C, Rubio A. Single-Walled Carbon Nanotube-Polymer Composites: Strength and Weakness. Advanced Materials, 2000; 12: 750-753.
4. Gong X, Liu J, Baskaran S, Voise R D, Young J S. Surfactant-Assisted Processing of Carbon Nanotube/Polymer Composite. Chemistry of Materials, 2000; 12: 1049-1052.
5. Haggenmueller R, Gommans H H, Rinzler A G, Fischer J E, Winey K I. Aligned Single-Walled Carbon Nanotubes in Composites by Melt Processing Methods. Chemical Physics Letters, 2000; 330: 219-225.
6. Qian D, Dickey E C, Andrews R, Rantell T. Load Transfer and Deformation Mechanisms in Carbon Nanotube-Polystyrene Composites. Applied Physics Letters, 2000; 76(20): 2868-2870.
7. Bower C, Rosen R, Jin L, Han J, Zhou O. Deformation of Carbon Nanotubes in Nano-tube Composites. Applied Physics Letters, 1999; 74(22): 3317-3319.

8. Jia Z, Wang Z, Xu C, Liang J, Wei B, Wu D, Zhu S. Study on Poly(Methyl Methacrylate)/Carbon Nanotube Composites. Materials Science and Engineering A, 1999; A271: 395-400.
9. Shaffer M S P, Windle A H. Fabrication and Characterization of Carbon Nanotube/Poly(vinyl alcohol) Composites. Advanced Materials, 1999; 11(11): 937-941.
10. Jin L, Bower C, Zhou O. Alignment of Carbon nanotubes in a Polymer Matrix by Mechanical Stretching. Applied Physics Letters, 1998; 73: 1197-1199.
11. Lourie O, Wagner H D. Transmission Electron Microscopy Observations Fracture of Single-Wall Carbon nanotubes Under Axial Tension. Applied Physics Letters, 1998; 73: 3527-3529.
12. Schadler L S, Giannaris S C, Ajayan P M. Load Transfer in Carbon Nanotube Epoxy Composites. Applied Physics Letters, 1998; 73(26): 3842-3844.
13. Wagner H D, Lourie O, Feldman Y, Tenne R. Stress-Induced Fragmentation of Multiwall Carbon Nanotubes in a Polymer Matrix. Applied Physics Letters, 1998; 72: 188-190.
14. Baughman R H. Putting a New Spin on Carbon Nanotubes. Science, 2000; 290: 1310-1311.
15. Gommans H H, Alldredge J W, Tashiro H, Park J, Magnuson J, Rinzler A G. Fibers of Aligned Single-Walled Carbon Nanotubes: Polarized Raman Spectroscopy. Journal of Applied Physics, 2000; 88(5): 2509-2514.
16. Vigolo B, Penicaud A, Coulon C, Sauder C, Pailler R, Journet C, Bernier P, Poulin P. Macroscopic Fibers and Ribbons of Oriented Carbon Nanotubes. Science, 2000; 290: 1331-1334.
17. Jiang K, Qunqing L, Fan S. Spinning Continuous Carbon Nanotube Yarns. Nature, 2002; 419: 801.
18. Vigolo B, Poulin P, Lucas M, Launois P, Bernier P. Improved Structure and Properties of Single-Wall Carbon Nanotube Spun Fibers. Applied Physics Letters, 2002; 81(7): 1210-1212.
19. McCullough R L. Micro-Models for Composite Materials - Continuous Fiber Composites. In: Delaware Composites Design Encyclopedia-Volume 2: Micromechanical Materials Modeling, Whitney J M, McCullough R L, Editors. Lancaster, PA: Technomic Pub. Co., 1990.
20. McCullough R L. Micro-Models for Composite Materials - Particulate and Discontinuous Fiber Composites. In: Delaware Composites Design Encyclopedia-Volume 2: Micromechanical Materials Modeling, Whitney J M, McCullough R L, Editors. Lancaster, PA: Technomic Pub. Co., 1990.
21. Odegard G M, Gates T S, Wise K E, Park C, Siochi E J. Constitutive Modeling of Nanotube-Reinforced Polymer Composites. Composites Science and Technology, 2003; 63: 1671-1687.
22. Rappe A K, Casewit C J. Molecular Mechanics Across Chemistry. Sausalito, California: University Science Books, 1997.
23. Pipes R B, Hubert P. Helical Carbon Nanotube Arrays: Mechanical Properties. Composites Science and Technology, 2002; 62: 419-428.
24. Pipes R B, Hubert P. Scale Effects in Carbon Nanostructures: Self-Similar Analysis. Nano Letters, 2003; 3(2): 239-243.
25. Odegard G M, Frankland S J V, Gates T S. *The Effect of Chemical Functionalization on Mechanical Properties of Nanotube/Polymer Composites*. in *44th*

AIAA/ASME/ASCE/AHS/ASC Structures, Structural Dynamics, and Materials Conference. 2003. Norfolk, VA.
26. Odegard G M, Gates T S, Nicholson L M, Wise K E. Equivalent-Continuum Modeling of Nano-Structured Materials. Composites Science and Technology, 2002; 62(14): 1869-1880.
27. Hashin Z, Rosen B W. The Elastic Moduli of Fiber-Reinforced Materials. Journal of Applied Mechanics, 1964; 31: 223-232.
28. Mori T, Tanaka K. Average Stress in Matrix and Average Elastic Energy of Materials with Misfitting Inclusions. Acta Metallurgica, 1973; 21: 571-574.
29. Benveniste Y. A New Approach to the Application of Mori-Tanaka's Theory in Composite Materials. Mechanics of Materials, 1987; 6: 147-157.
30. Popov V N, Van Doren V E, Balkanski M. Elastic Properties of Crystals of Single-Walled Carbon Nanotubes. Solid State Communications, 2000; 114: 395-399.
31. Bogetti T A, Gillespie J W. Process-Induced Stress and Deformation in Thick-Section Thermoset Composite Laminates. Journal of Composite Materials, 1992; 26(5): 626-660.
32. Hull D, Clyne T W. An Introduction to Composite Materials. Cambridge: Cambridge University Press, 1996.

Table 1. Elastic properties of effective fiber

G_T^f = 4.4 GPa
K_T^f = 9.9 GPa
G_L^f = 27.0 GPa
Y_L^f = 450.4 GPa
C_L^f = 457.6 GPa

Table 2. Scale input parameters

Scale	**Diameter (m)**	**Matrix**	**V_f**
SWCN	1.38×10^{-9}	-	-
nano-array	1.48×10^{-8}	none	79%
nano-wire	1.69×10^{-7}	polymer	70%
micro-fiber	1.93×10^{-6}	polymer	54.6%
lamina	2.20×10^{-5}	polymer	33.2%

Table 3. SWCN geometric properties

Outside Diameter (D_o)	1.38 x 10^{-9} m
Inside Diameter (D_i)	0.73 x 10^{-9} m
Wall Thickness (t)	0.33 x 10^{-9} m
Length	4.8 x 10^{-7} m
Nanotube Spacing (s)	1.48 x 10^{-9} m
Maximum Packing	79 %

Table 4. SWCN array properties.

$E_L^{s\,*}$	650 GPa
$E_T^{s\,*}$	16.1 GPa
$G_{LT}^{s\,**}$	5.80 GPa
$G_{NT}^{s\,**}$	5.80 GPa
$\nu_{LT}^{s\,*}$	0.16
$\nu_{NT}^{s\,**}$	0.40

* From Popov. *et al*. [30]

** Assumed by authors.

Table 5. SWCN volume fractions for each concentration

Concentration	Volume fraction (%)
dilute	< 0.01
semi-dilute	0.01-1.0
concentrated	1.0-19.6
hyper-concentrated	> 19.6

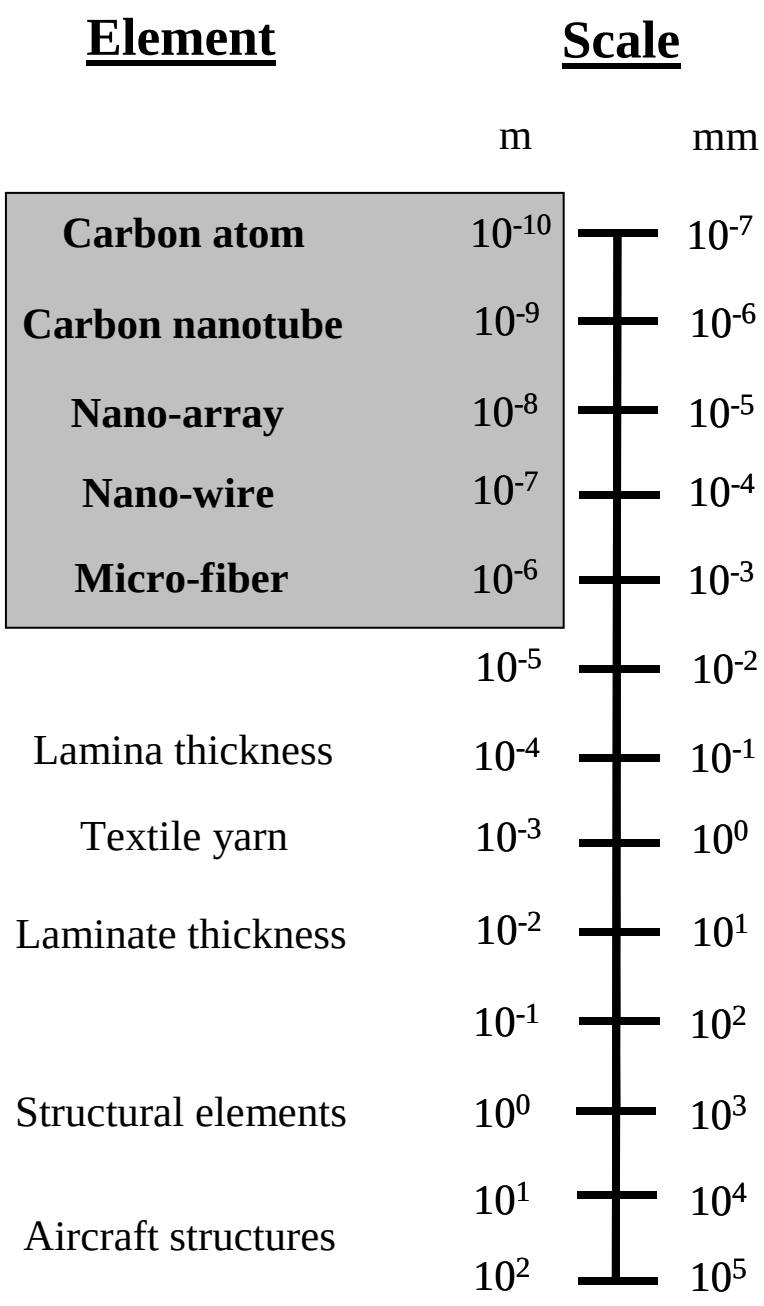

Fig. 1. Geometric scale versus structural feature

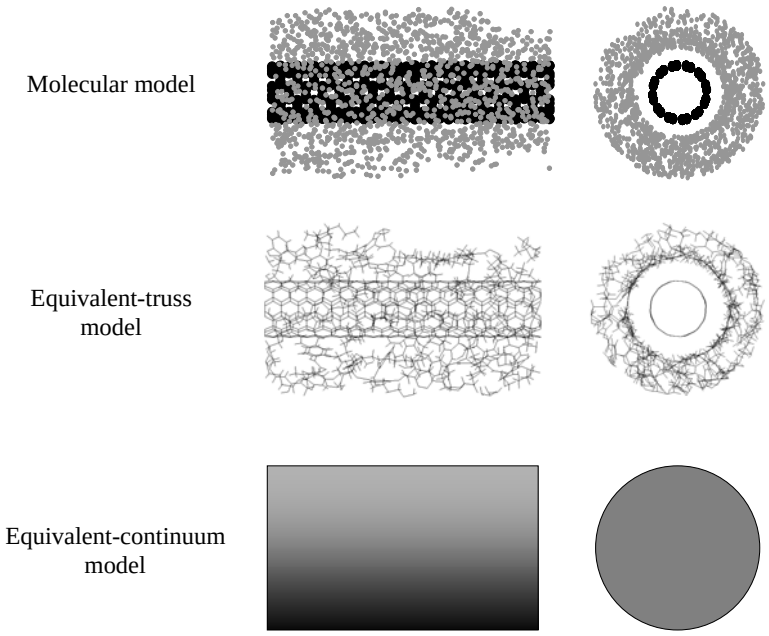

Fig. 2. Representative volume elements of molecular, equivalent-truss, and equivalent-continuum models

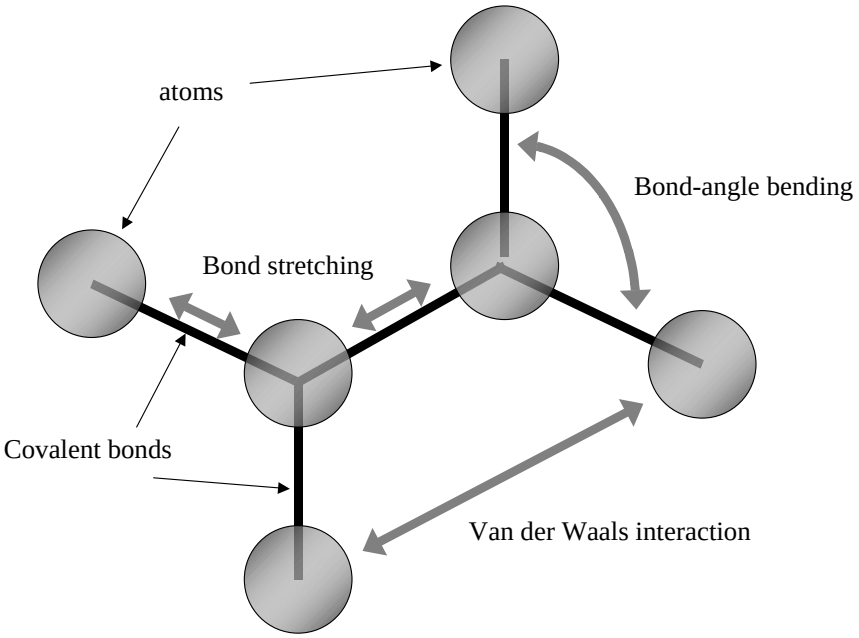

Figure 3. Molecular mechanics modeling

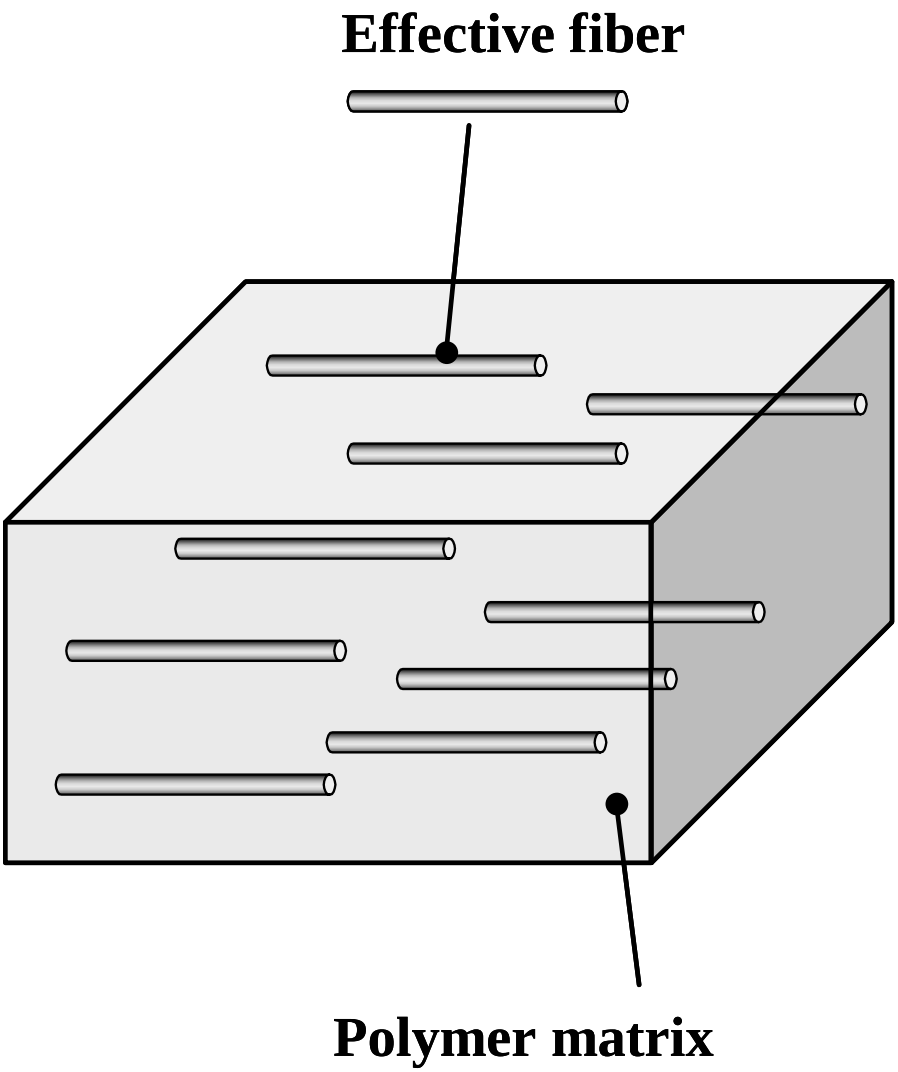

Fig. 4. Orientation of effective fiber in a polymer composite

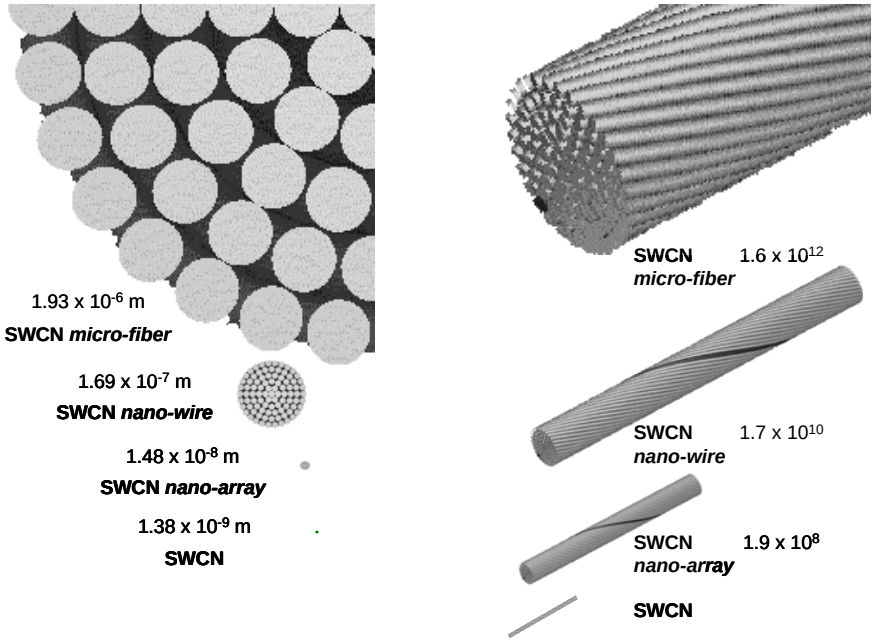

Fig. 5. a) Self-similar scales and b) number of SWCN per meter length

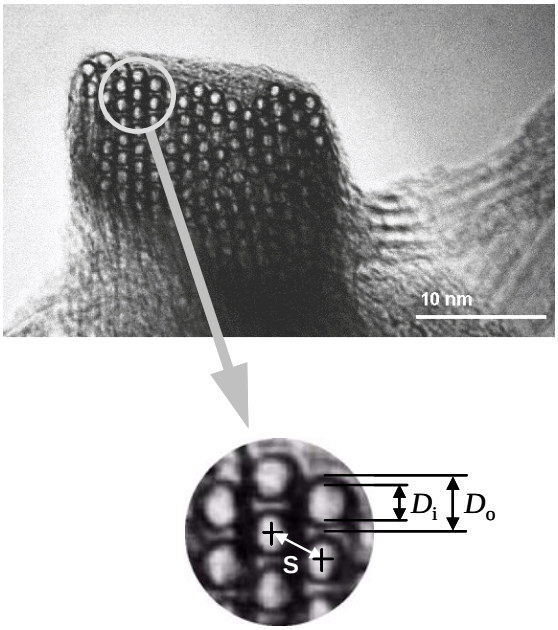

Fig. 6. SWCN array image analysis

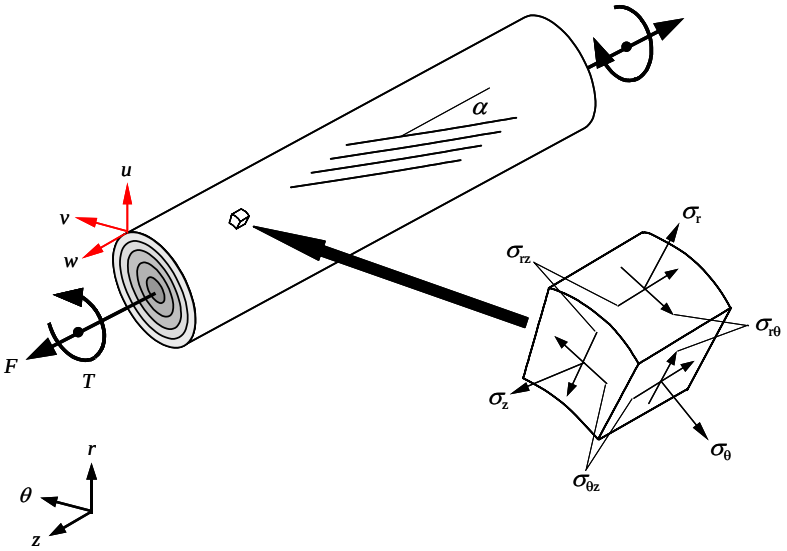

Fig. 7. Layered cylinder nomenclature

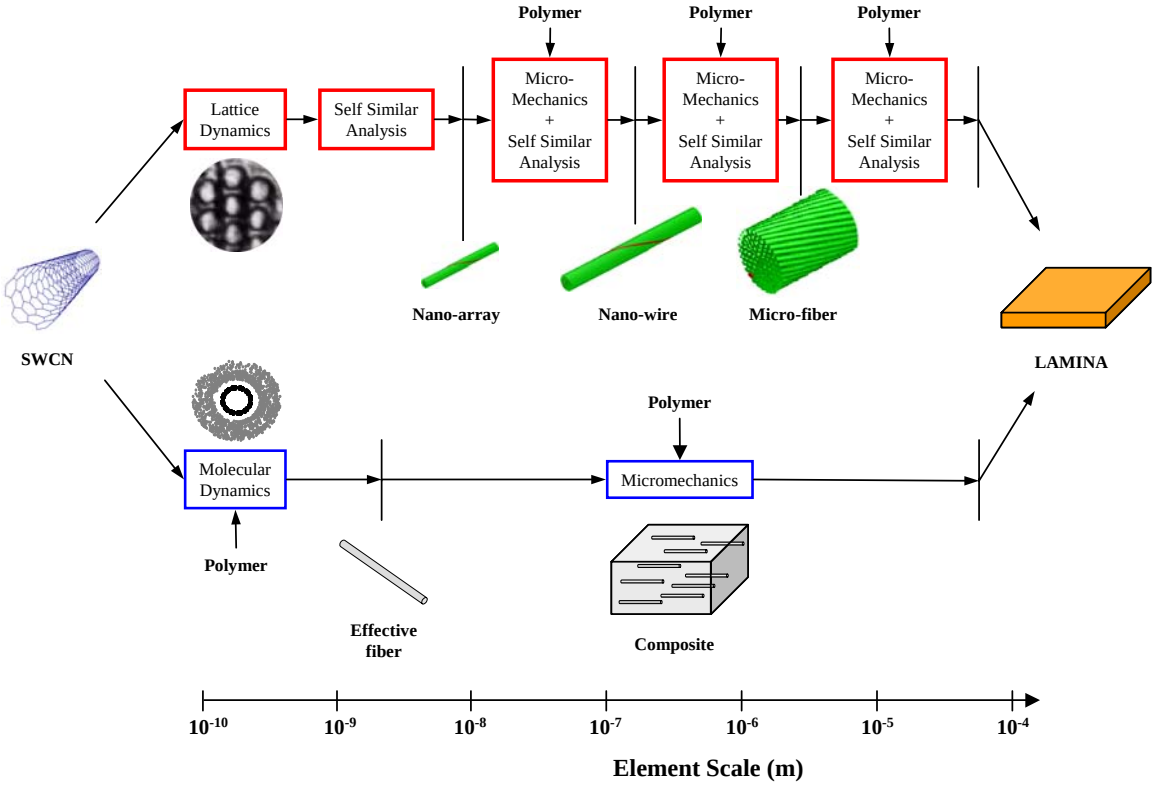

Fig. 8. SWCN/polymer composite modeling approaches

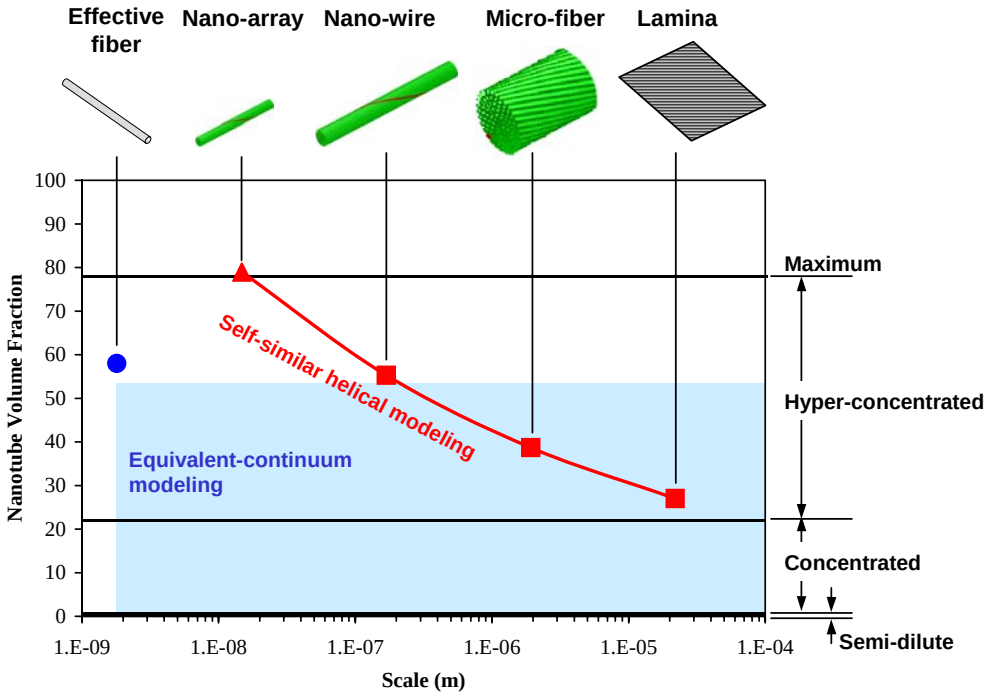

Fig. 9. SWCN volume fraction and scale relationship for different nanocomposite elements

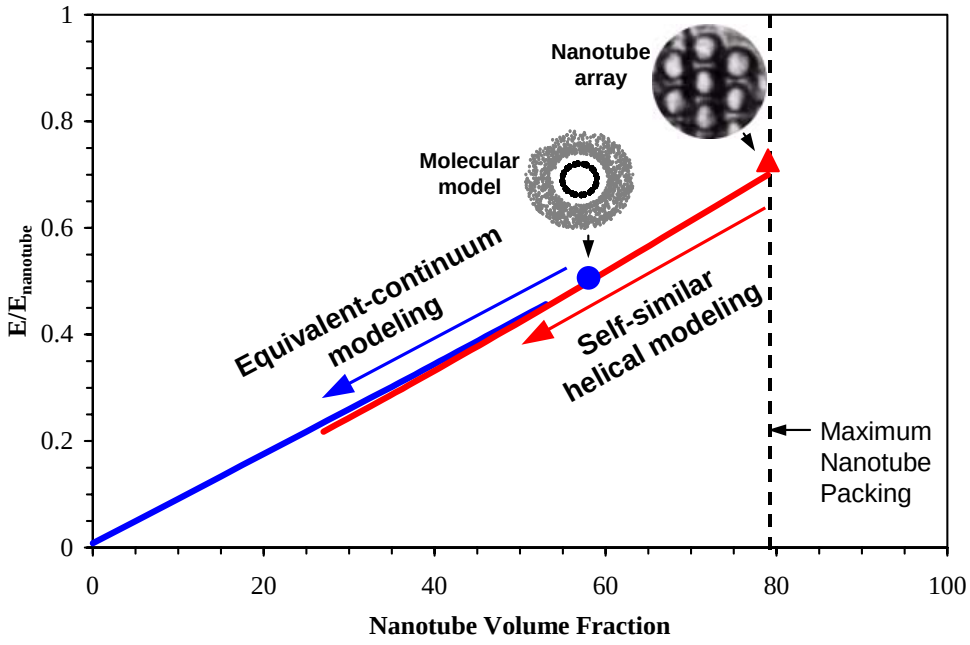

Fig. 10. Predicted modulus for SWCN polymer composite